ACI STRUCTURAL JOURNAL TECHNICAL PAPER

Title no. 104-S09

Effectiveness of Fiber-Reinforced Polymer in Reducing Corrosion in Marine Environment

by Kwangsuk Suh, Gray Mullins, Rajan Sen, and Danny Winters

This paper presents results from a long-term study that evaluated the role of fiber-reinforced polymer (FRP) in reducing the corrosion rate in a marine environment. Twenty-two 1/3-scale models of prestressed piles cast with built-in chloride were exposed to simulated tidal cycles under outdoor ambient conditions for nearly 3 years. These included eight carbon FRP (CFRP), eight glass FRP (GFRP)-wrapped specimens, and six controls. Embedded titanium reference electrodes and thermocouples were used to monitor the corrosion performance inside the wrapped region throughout the exposure period. The performance of the FRP was evaluated on the basis of bond and gravimetric tests conducted at the end of the exposure period. The results showed that the FRP-concrete bond was largely unaffected by exposure and both CFRP and GFRP-repaired specimens significantly outperformed the controls. The underlying trend in corrosion rate measurements showed increases for the controls and reductions for the wrapped specimens. This was reflected by much lower metal losses in wrapped specimens compared with controls. Overall, the study showed that FRP is effective in mitigating corrosion in a marine environment.

Keywords: bond; corrosion; prestress; reinforcement; test.

INTRODUCTION

The poor performance of conventional repairs has led to renewed interest in the application of fiber-reinforced polymer (FRP) materials for rehabilitating corroded concrete structures. Despite higher material costs, FRP repairs may be more economical if they result in a reduction in re-repairs that is often the reality for corrosion repair. Several highway agencies have explored this option over the past decade. In 1994, the Vermont Transportation Agency opted to use FRP over conventional methods for repairing corrosion-damaged columns because it resulted in 35% cost savings.[1] For the same reason, the New York State Department of Transportation (NYDOT) chose FRP for repairing corrosion-damaged columns.[2] More examples may be found in a recent state-of-the-art paper.[3]

The role of FRP in mitigating corrosion has been the subject of several investigations.[3] The majority of the studies[4-8] focused on applications relating to corrosion damage in reinforced concrete elements in cold regions caused by salt water run-off from faulty expansion joints. There have been fewer studies relating to corrosion mitigation in tidal waters under hot, humid conditions[9-12] where corrosion rates are significantly higher. Such applications have only become possible[13-16] because of the availability of new resins that can cure in water.

In 2001, the Florida and U.S. Department of Transportation funded a 44-month study to investigate the use of FRP for the underwater repair of prestressed piles. The study included both laboratory testing and field demonstrations. This paper provides details of a long-term exposure study conducted to assess the role of FRP in mitigating corrosion. In the study, instrumented, 1/3-scale models of carbon FRP (CFRP) and glass FRP (GFRP) wrapped prestressed piles were exposed to simulated tidal cycles under outdoor ambient conditions for nearly 3 years. The performance of the FRP was assessed in comparison to identical unwrapped specimens that were placed in the same environment through gravimetric testing. Complete details may be found in the final report.[12]

RESEARCH SIGNIFICANCE

This paper provides quantitative data on the performance of FRP in reducing corrosion under exposure comparable to natural conditions. The use of embedded reference electrodes permitted the corrosion performance of the FRP wrapped region to be monitored throughout the exposure. Comparative data on the actual metal loss in identically exposed wrapped and unwrapped specimens is helpful for highway agencies in assessing the efficacy of FRP in corrosion mitigation applications.

OBJECTIVES

The overall goal of the research project was to evaluate the effectiveness of FRP in slowing down corrosion in heavily chloride-contaminated prestressed concrete elements that are characteristic of a marine environment. Both carbon and fiberglass were tested and the role of number of fiber layers investigated. Effectiveness was evaluated by monitoring corrosion rate and by gravimetric testing in which the actual metal loss in strands and ties retrieved from exposed specimens was determined.

EXPERIMENTAL PROGRAM

As corrosion is a slow process, two broad strategies have been used for accelerating corrosion. In the first method, electrochemical reactions responsible for corrosion are simulated by applying appropriate corrosion currents using either a constant voltage or a constant current system. In the second method, acceleration is achieved by using permeable, high water-cement mixtures, heat, or by casting specimens with chlorides. Specimens are subsequently exposed to simulated tidal cycles and subjected to alternate drying and wetting. Acceleration may be achieved by manipulating the relative lengths of the dry and wet cycles. By making the dry cycle longer, accessibility of oxygen is enhanced that can

ACI Structural Journal, V. 104, No. 1, January-February 2007.
MS No. S-2006-110 received March 14, 2006, and reviewed under Institute publication policies. Copyright © 2007, American Concrete Institute. All rights reserved, including the making of copies unless permission is obtained from the copyright proprietors. Pertinent discussion including author's closure, if any, will be published in the November-December 2007 *ACI Structural Journal* if the discussion is received by July 1, 2007.

ACI member **Kwangsuk Suh** *is a Structural Engineer at Parsons Brinckerhoff Quade and Douglas, Inc., Tampa, Fla. He received his PhD from the Department of Civil and Environmental Engineering at the University of South Florida, Tampa, Fla.*

Gray Mullins *is an Associate Professor of structural engineering at the University of South Florida. His research interests include full-scale testing and instrumentation of structures and foundations.*

Rajan Sen, *FACI, is a Professor of structural engineering at the University of South Florida. He is a member of ACI Committees 215, Fatigue of Concrete; 440, Fiber Reinforced Polymer Reinforcement; and 444, Experimental Analysis for Concrete Structures. His research interests include fiber-reinforced polymers.*

Danny Winters *is a Research Associate and a PhD student in the Department of Civil and Environmental Engineering at the University of South Florida. His research interests include full-scale testing of foundations.*

accelerate the corrosion process. The first approach yields results more quickly. The second is slower, but corrosion products and processes are more representative of naturally occurring corrosion.

In this study, the second approach was adopted in which specimens were exposed to simulated tidal cycles under outdoor ambient conditions. The wet-dry cycles were kept the same but the exposure period made sufficiently long so that the difference in the performance of wrapped and unwrapped specimens would become apparent.

Specimen details

The specimens used in the study were 1/3-scale model of 45 cm (18 in.) square prestressed piles that had been identified in earlier studies as being the most common and, therefore, most commonly found to have exhibited corrosion damage. The 15 x 15 x 152 cm (6 in. x 6 in. x 5 ft) long specimens were prestressed by four 8 mm (5/16 in.), seven-wire, low relaxation 1860 MPa (Grade 270) strands (Fig. 1). This configuration ensured that the effective prestress in the model piles exactly matched that in the prototype when stressed to code-specified stressing levels. The central fifth strand shown in Fig. 1 was unstressed and served as a counter electrode for linear polarization tests that were used to monitor the corrosion rate in the steel.

A 55 cm (22 in.) length corresponding to 1.67 m (66 in.) splash zone in the prototype was fabricated with 3% of chloride ion by weight of cementitious material. This left 48 cm (19 in.) of regular concrete both above and below that was sufficient for full prestress force transfer ($50d_b$ = 39.6 cm [15.6 in.]).

Specimens were cast all at once in a single line in a specially adapted prestressing bed at a commercial facility. As a result, the prestressing forces and concrete mixtures were identical for all specimens. Wood trims with a radius of 13 mm (1/2 in.) were inserted along the bottom corners of the form to ensure that there no sharp corners at these locations. The edges at the top were finished using a 7.5 cm (3 in.) wide edging trowel so that these edges were also curved. This greatly reduced the preparation work required in subsequent wrapping.

Instrumentation

The prestressing forces at the live and dead ends were monitored during fabrication of the specimen to ensure that the final effective stresses were consistent with those in the prototype pile. Embedded activated titanium reference electrodes and thermocouples were installed at pre-designated locations as shown in Fig. 1.

Embedded reference electrodes ensured greater reliability of the corrosion measurements (when compared with surface

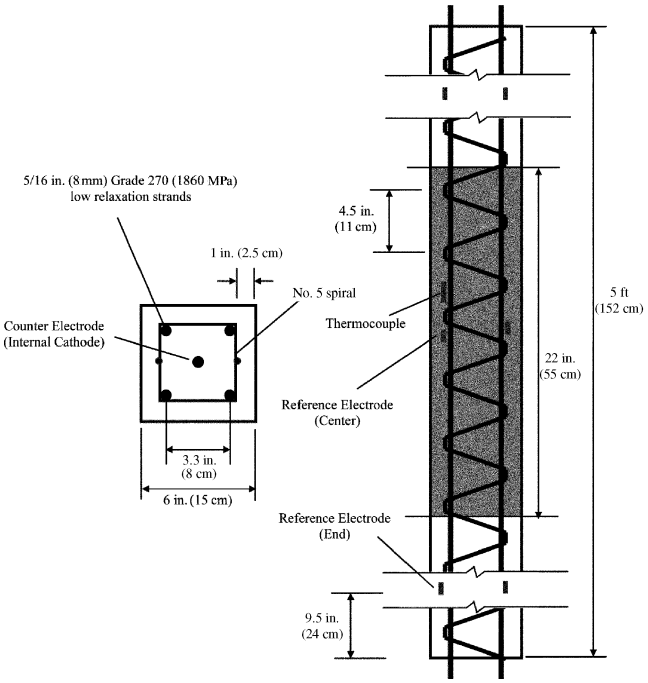


Fig. 1—Specimen geometry.

measurements) by eliminating environmental effects due to changes in the temperature and humidity of the surface. More importantly, it allowed potential measurements inside the wrapped region to be readily made without the need for cutting through the wrap to expose the concrete surface. Thermocouples enabled changes in corrosion rate with temperature to be assessed.

Concreting

The concrete placement was conducted in two phases: a regular FDOT Class V special mixture was first placed, vibrated, and finished followed by a second batch in which a measured amount of the chloride admixture[12] was added to the concrete mixer, rotated, and placed between sheet metal barriers (dams) that were removed subsequently. The specimens were covered by a plastic sheet and allowed to cure. The average compressive strength at the time of release was 41.7 MPa (6.05 ksi) for the regular concrete and 34.3 MPa (4.98 ksi) for the chloride contaminated concrete.

Wrap details

The goal of the study was to evaluate the performance of FRP in specimens where the chloride threshold had been exceeded, but there was no visible sign of corrosion. For this reason, 16 specimens were wrapped when the concrete was 28 days old. FRP was applied over a 0.91 m (36 in.) length in the central region of the specimen. This meant that it extended 17.5 cm (7 in.) above and below the boundary of the 55 cm (22 in.) chloride contaminated region (Fig. 1). Eight specimens were wrapped with bidirectional CFRP using bidirectional CFRP system. Eight others were wrapped using a bidirectional GFRP and epoxy.

Material properties of the epoxies and the FRP provided by the manufacturers are summarized in Table 1 and 2. The number of FRP layers varied from 1 to 4 and the recommended lap length was provided. This was 5 cm (2 in.) for CFRP and 15 cm (6 in.) for GFRP. To protect the FRP wrap



Fig. 2—Outdoor exposure specimens.

Table 1—Material properties of epoxies

Properties	CFRP (MAS 2000)	GFRP (Tyfo® S)
Tensile strength, ksi (MPa)	45.2 (312)	10.5 (72)
Tensile modulus, ksi (MPa)	2620 (18,064)	461 (3178)
Flexural strength, ksi (MPa)	62.3 (430)	11.5 (79)
Flexural modulus, ksi (MPa)	2560 (17,651)	400 (2758)
Elongation, %	1.96	5

Table 2—Material properties of FRP

Property	Values	
	CFRP	Tyfo® Web
Tensile strength, ksi (MPa)	90 (621)	44.8 (309)
Modulus of elasticity, ksi (MPa)	10,600 (73,084)	2800 (19,305)
Elongation at break, %	1.2	1.6
Thickness, in. (mm)	0.020 (0.508)	0.01 (0.254)

Table 3—Details of test specimens

Specimen type	Specimen ID	Wrap layers	Reference electrodes
Outdoor control	No. 38, 39, 40	0	2
	No. 41		6
Indoor control	No. 42		2
	No. 43		6
CFRP wrap	No. 52, 56	1	2
	No. 53	2	
	No. 54, 58	3	
	No. 55	4	
	No. 57	2	6
	No. 59	4	
GFRP wrap	No. 44, 48	1	2
	No. 45	2	
	No. 46, 50	3	
	No. 47	4	
	No. 49	2	6
	No. 51	4	

from ultraviolet radiation, two coats of external latex paint were applied over the wrapped area.

TIDAL SIMULATION SETUP

Twenty specimens (16 wrapped and four unwrapped controls) were placed upright inside a 1.82 x 3.04 x 1.22 m (6 x 10 x 4 ft) tank, which was kept outdoors (Fig. 2). Two unwrapped specimens were placed in an indoor tank in a controlled environment and served as indoor controls. Details are summarized in Table 3.

All outdoor and indoor specimens were subjected to simulated tidal cycles in 3.5% salt water (Fig. 2). The variation in water depth was modeled for the Tampa Bay region where the difference between high and low tide is approximately 45 cm (18 in.). The water level at high tide was 80 cm (32 in.) from the bottom. It was 35 cm (14 in.) at low tide. The tide was changed every 6 hours and was controlled by a water pump and floating switch. This ensured that a 5 cm (2 in.) length of the wrap was permanently submerged in water. This type of exposure had the maximum chance of trapping moisture within the wrap. Such entrapment of moisture had been observed in a study conducted by the University of Texas at Austin.[17]

Specimens were exposed to this environment for nearly 3 years at which time they were removed for detailed examination and analysis that included measurement of metal loss in wrapped and unwrapped specimens by gravimetric testing.

CORROSION MONITORING

Half-cell potential measurements were taken using a high impedance voltmeter. The embedded titanium reference electrodes were calibrated against a copper-copper sulfate reference electrode (CSE) and all results reported are with respect to these electrodes. Potential measurements were regularly made with the first reading taken 24 days after the specimens had been cast. Initially, measurements were taken weekly but became less frequent as readings stabilized following prolonged exposure.

Linear polarization measurements were made using a PR monitor. This has a three-electrode probe comprising a reference, working, and counter electrode. The central strand provided in the specimen (Fig. 1) served as the counter electrode. The PR monitor measures the polarization resistance that is inversely proportional to the corrosion rate in the steel. In the calculations, the polarized area was assumed to be the same as the chloride-contaminated area (55 cm [22 in.] length). Concrete resistivity was measured using a soil-resistance meter.

All thermocouples embedded in the concrete were hooked to a data acquisition system. Temperature data was measured and recorded every hour. Connections to the steel and the titanium reference electrodes for the corrosion measurements were placed inside a weatherproof box (Fig. 3) that allowed readings to be readily taken.

RESULTS

Half-cell potentials

Figure 4 provides an overview of the variation in the averaged half-cell potential (relative to copper-copper sulfate) measured at midheight, that is, at the center of the wrapped region for all the controls (four outdoors and two indoors) and the wrapped specimens (eight CFRP and eight GFRP). Wrapping was conducted on the 28th day and wet-dry cycles started on the 111th day after casting when the simulated tidal setup became operational.

All readings were more negative than –350 mV indicating that there was a 90% probability of corrosion. The readings became much more negative immediately after the start of wet-dry cycles possibly because of the availability of water. For the specimens kept outdoors, potential changes were broadly similar for the first 350 days. After this time period, however, there was a divergence in the potential values with



Fig. 3—Weatherproof measurement box.

the unwrapped control specimens becoming more negative and the FRP wrapped specimens becoming less negative. This change in readings coincided with the appearance of cracks along the strand line and the formation of corrosion products around cracks on the surface of the unwrapped control specimens (Fig. 5). There was no similar evidence of damage in any of the wrapped specimens. Nor were the readings for CFRP and GFRP significantly different. Additional results[12] showed that the number of FRP layers had a relatively minor effect on the potential readings.

Corrosion rate results

Linear polarization measurements were taken at midheight where corrosion rates were expected to be the highest. Figure 6 provides an overview of all the results as well as the temperature variation. Each corrosion rate data point represents the average for that type of specimen (for example, eight CFRP, eight GFRP, two indoor controls, or four outdoor controls). Additional plots showing individual results may be found in the final report.[12]

The corrosion rate in Fig. 6 is expressed in mm/year. Inspection of Fig. 6 shows that while corrosion rates in all specimens declined during the period between wrapping and exposure to the simulated tidal cycles, the underlying trend in the subsequent results was an increase in the corrosion rate in the controls and a decrease in the rate in the wrapped specimens. Undulations in the corrosion rate were largely due to variations in the ambient temperature at the time the reading was taken (always at low tide) and were more prominent in the outdoor controls when compared to the indoor specimens. The temperature of the indoor controls was unfortunately not constant, but rather maintained for laboratory occupant comfort (near 25 °C [77 °F]) and would have fluctuated somewhat with the outdoor conditions. There was little difference between the corrosion rates in the CFRP and GFRP wrapped specimens; temperature-induced changes in corrosion rate were likewise apparent. Such temperature-induced corrosion rate variations are not surprising given the electrochemical nature of the corrosion process.

The average corrosion rate in the controls was 0.018 mm/year at the end of the exposure period. The wrapped specimens show approximately 1/3 of this magnitude at 0.0055 mm/year. These values are commensurate with corrosion rates where visible damage can be expected in 2 to 10 years.[18]

EFFECT OF EXPOSURE ON BOND

Following conclusion of the exposure, test specimens were removed from the tanks for further evaluation and

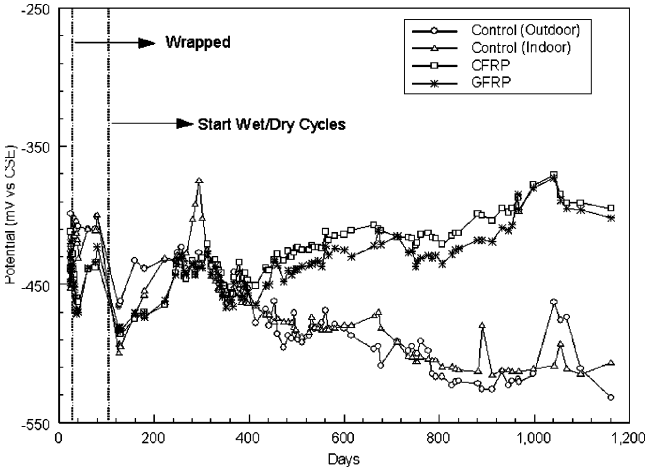


Fig. 4—Result of half-cell potential measurements.



Fig. 5—Surface cracks on unwrapped specimens.

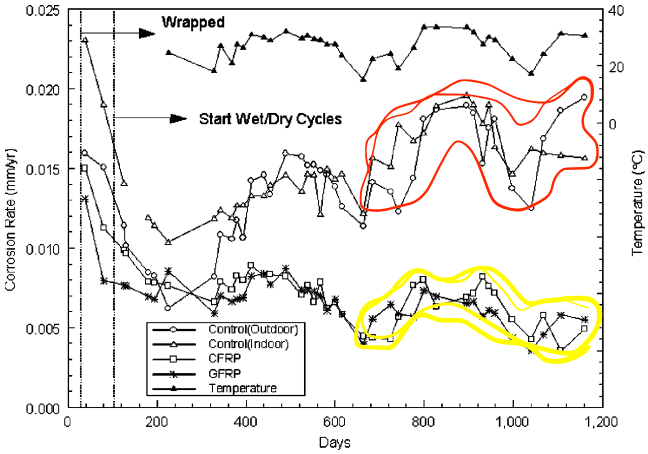


Fig. 6—Result of linear polarization tests.

testing. This included bond tests on the wrapped specimens, crack mapping of the controls, and gravimetric testing to quantify metal loss.

The bond between FRP and concrete was determined from pull-out tests carried out in accordance with ASTM D 4541[19] using an adhesion tester. The tester used 3.6 cm (1.456 in.) diameter aluminum dollies. A total of eight wrapped specimens were tested: four CFRP specimens (No. 54, No. 55, No. 56, and No. 57) and four GFRP (No. 47, No. 48, No. 50, and No. 51) with one, two, three, or four FRP layers.

The tests were performed on two faces of each specimen and at three locations per face (Fig. 7). The three levels



Fig. 7—Bond test.

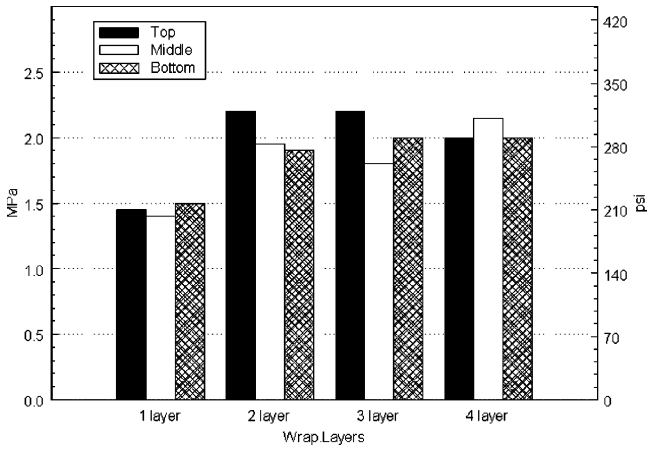


Fig. 8—Bond test results for CFRP wrap.

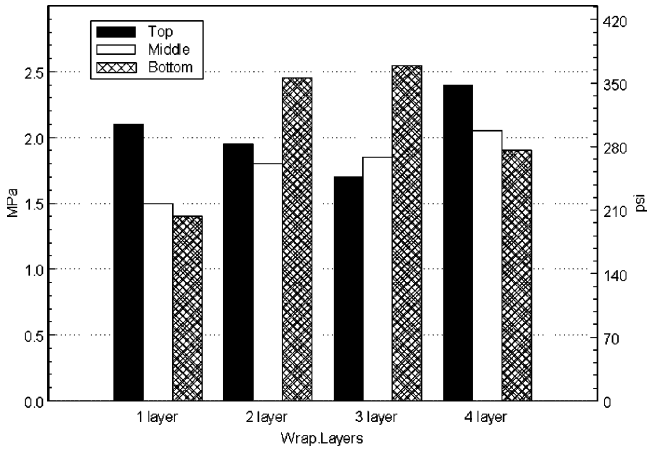


Fig. 9—Bond test results for GFRP wrap.

selected were the dry zone (top), tidal zone (middle), and the submerged zone (bottom).

The results of the bond tests for the CFRP- and GFRP-wrapped specimens are summarized in Fig. 8 and 9, respectively. The bond strength of CFRP specimens varied from 1.4 to 2.2 MPa (203 to 319 psi) and those for the GFRP specimens from 1.4 to 2.6 MPa (203 to 370 psi). Most of the bond failures in the top and middle locations occurred in the concrete indicating that the bond was good. In the submerged zones, however, failure occurred in the epoxy.

The average bond strength at these three levels considering all the specimens varied from 1.8 to 2.0 MPa (265 to 285 psi) in CFRP specimens and from 1.8 to 2.1 MPa (261 to 301 psi) in GFRP specimens. Thus, the average bond strength was marginally higher in the glass-fiber specimens in comparison to the carbon fiber specimens.

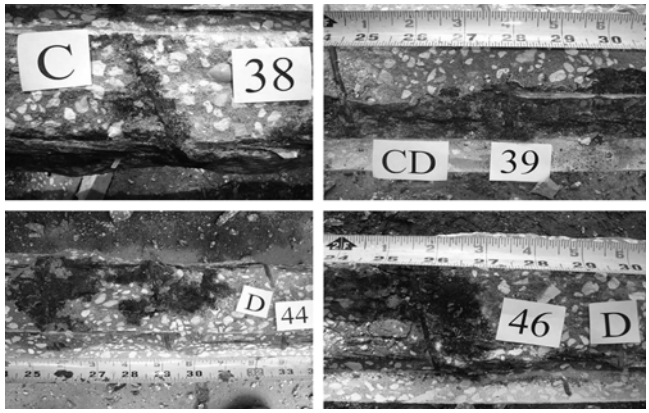


Fig. 10—Exposed steel of unwrapped specimens.

Although epoxy failure was the most commonly occurring mode in the submerged region, the measured ultimate bond stress was not significantly higher even where there was failure in the concrete. The bond strength was also unaffected by the number of FRP layers indicating that the inter-layer bond was good and the material was properly bonded in the first place. The somewhat poorer performance in the submerged region is not a result of the installation method as all specimens were dry-wrapped but rather is more likely a consequence of ingress of moisture into the resin over time.

GRAVIMETRIC TESTING

All 22 specimens were gravimetrically tested to determine the actual steel loss at the end of the 1160-day exposure period. As noted previously, the Texas study[17] reported that the FRP wrap had entrapped water that had led to increased corrosion inside the wrap. No similar entrapment was found in this study and no similar localized corrosion was observed.

The strands and ties were extracted by making longitudinal cuts on the concrete surface with an electric saw and subsequently carefully chipping the cover off to expose the steel (Fig. 10 and 11). Inspection of these figures shows that there was much greater corrosion in the unwrapped controls than in the wrapped specimens. In the wrapped specimens, there was no evidence of corrosion products in some specimens unlike that in the unwrapped controls where corrosion products were always present.

The prestressing strands and ties were carefully extracted from all the specimens. The central-most section of the strands were cut to 0.91 m (36 in.) lengths, labeled, and numbered. The strands and ties were stored in sealed bags for subsequent cleaning. In the cleaning process, the strands were disassembled into seven separate wires to ensure there was no trapped rust.

A summary of the measured steel loss from all the results is shown in Table 4. Because the target area contaminated with chloride was 55 cm long (22 in.), located in the central portion of the specimen (Fig. 1), the steel loss was assumed to have occurred only in the chloride-contaminated region. The total loss in all four strands and ties was averaged for each specimen and compared with the controls.

It may be seen from Table 4 that the average steel loss in strands and ties in outdoor and indoor unwrapped specimens were similar (6.6 and 10.1% versus 6.6 and 8.9%). This suggests that temperature and humidity variation did not make as much a difference. Thus, corrosion gains made in the outdoor specimens during summer and fall were offset

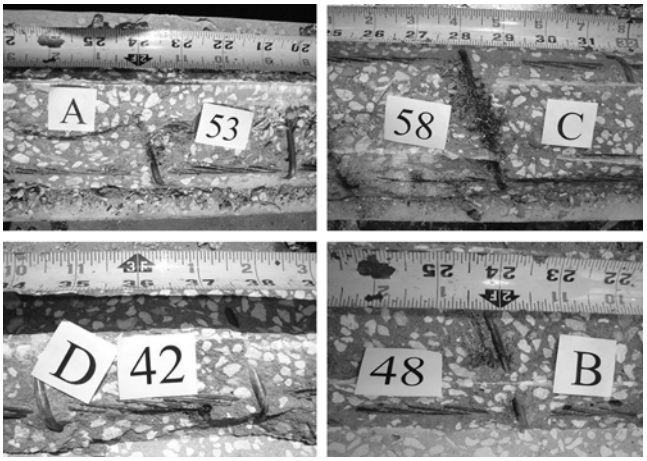


Fig. 11—Exposed steel of wrapped specimens.

Table 4—Averaged metal loss

Specimen type	Layer	Metal loss, %	
		Strand	Tie
Outdoor	0	6.6	10.1
Indoor	0	6.6	8.9
CFRP	1	3.5	7.1
	2	3.1	5.7
	3	3.4	6.9
	4	3.3	6.9
	Average	3.3	6.6
GFRP	1	3.6	6.7
	2	3.3	6.2
	3	3.5	5.9
	4	3.3	6.5
	Average	3.4	6.3

by lower corrosion rates in winter and spring. In contrast, the fluctuations in the corrosion rate in specimens kept inside the laboratory were smaller.

The performance of the wrapped specimens was much better as is evident from Fig. 10 and 11. The average metal loss in strands was 3.3% for CFRP and 3.4% for GRFP, approximately half that of the 6.6% in the controls. For the ties, average metal loss was 6.6% for carbon and 6.3% for glass compared with 10.1% for the outdoor controls (Table 4).

Aside from the difference in metal loss, there were 30 breaks in individual wires making up the strands in the six unwrapped specimens (average five breaks per pile) indicative of localized pitting corrosion. In contrast, there was only one instance of breakage in the 16 wrapped specimens (0.0625 breaks per pile). Thus, the averaged readings do not completely reflect the actual performance of the unwrapped specimens compared with the wrapped ones.

A more detailed breakdown of the gravimetric results showing the relationship between metal loss and number of FRP layers is given in Table 5. It may be seen from this table that the performance of the FRP did not necessarily improve as the number of layers increased. Overall, the results for carbon and glass were comparable.

DISCUSSION

The goal of this study was to evaluate the effectiveness of the FRP in slowing down the corrosion rate in specimens in which the chloride threshold for corrosion initiation had been exceeded prior to wrapping. Here, the passive layer protecting steel is destroyed; but there is no visible sign of corrosion. This condition is not uncommon and was encountered in recent field applications[14-16] where chloride levels in the cover were comparable to those used in the test specimens.

Table 5—Summary of gravimetric results

Specimen type		Specimen ID	Metal loss, %	
			Strand	Tie
Outdoor control		No. 38	6.3	11.7
		No. 44	7.6	9.8
		No. 45	6.4	9.7
		No. 46	5.9	9.1
		Average	6.6	10.1
Indoor control		No. 39	6.5	10.0
		No. 49	6.6	7.9
		Average	6.6	8.9
Carbon	1 layer	No. 54	3.4	6.8
		No. 58	3.6	7.3
		Average	3.5	7.1
	2 layers	No. 55	3.1	6.1
		No. 42	3.1	5.2
		Average	3.1	5.7
	3 layers	No. 56	3.3	6.7
		No. 59	3.5	7.1
		Average	3.4	6.9
	4 layers	No. 57	3.4	7.7
		No. 43	3.2	6.1
		Average	3.3	6.9
	Carbon average		3.3	6.6
Glass	1 layer	No. 48	3.5	6.4
		No. 52	3.6	6.9
		Average	3.6	6.7
	2 layers	No. 47	3.4	6.0
		No. 40	3.3	6.3
		Average	3.3	6.2
	3 layers	No. 50	3.7	6.4
		No. 53	3.3	5.4
		Average	3.5	5.9
	4 layers	No. 51	3.7	6.4
		No. 41	3.0	6.6
		Average	3.3	6.5
	Glass average		3.4	6.3

The outdoor exposure setup and the simulated tidal cycles were very similar to natural conditions under which corrosion occurs in a marine environment. By using multiple embedded reference electrodes, both corrosion potential and linear polarization rates could be readily measured at the critical midheight without compromising the integrity and continuity of the wrap. These measurements indicated that FRP slowed down but did not stop the corrosion rate. The performance of the CFRP and GFRP were comparable and largely independent of the number of wrapping layers. These findings were confirmed through destructive gravimetric testing where metal losses in wrapped specimens were measured to be significantly lower than its identical unwrapped counterpart.

The fact that FRP was unable to stop the corrosion process is not particularly surprising given that oxygen and moisture present inside the concrete prior to wrap were sufficient to sustain the electrochemical reaction. Given that there are

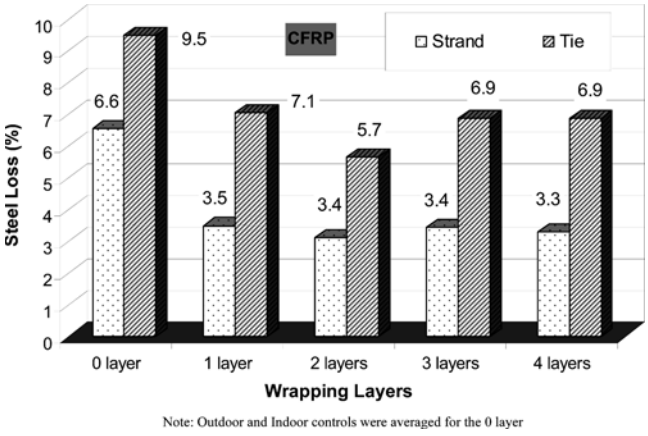


Fig. 12—Effect of CFRP wrap on maximum steel loss.

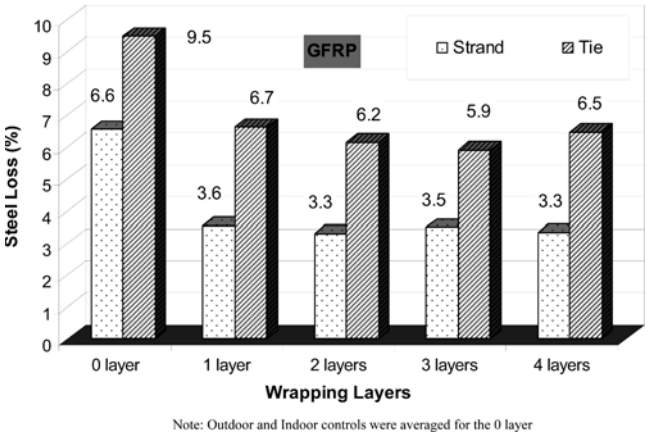


Fig. 13—Effect of GFRP wrap on maximum steel loss.

multiple pathways for transporting both these deleterious materials (from regions outside the wrapped area) through the pores in hardened concrete, it is unlikely that the corrosion can be stopped. As the FRP also confines the concrete, however, the confining pressures can compress the corrosion products and change the underlying electrochemical reactions. This may explain why trends in the corrosion rate measurements showed reductions in the corrosion rate over time (Fig. 6).

The surprising result was that two FRP layers were optimal regardless of the material (Table 5). Providing a larger number of layers provided increased strength but did not help corrosion mitigation. It provides further evidence that oxygen and moisture inside the wrap dictate the corrosion process. As results for one FRP layer were poorer, however, a minimum of two layers should be used in FRP corrosion mitigation applications.

A detailed examination of the profile of the corroded strand has not yet been made. Development work is currently underway to construct an automated system that can electronically record the profile of the strands. Once this has been completed, tests will be conducted to determine the stress-strain characteristics of the corroded strands. These findings will be reported at a future date.

CONCLUSIONS

Based on the results presented, the following conclusions may be drawn:

1. The measured metal loss in wrapped specimens was significantly lower than that in identical unwrapped controls exposed to the same environment. Both CFRP and GFRP were equally effective in drastically reducing the rate of corrosion but were nonetheless unable to stop corrosion even when four layers were used (Fig. 12 and 13);
2. The performance of CFRP and GFRP in slowing down the corrosion rate was comparable (Table 4). The linear polarization measurements correctly predicted this and also the underlying trends in the metal loss in wrapped and unwrapped specimens (Fig. 5);
3. The level of corrosion protection afforded by FRP does not increase with the number of FRP layers. In this study, two layers were found to be the optimal number based on gravimetric testing (Table 5 and Fig. 12 and 13);
4. The gravimetric testing method used to determine metal loss is not fully indicative of the severity of the structural impact of the damage as the metal losses. Localized corrosion led to breakages in 30 wires in the six unwrapped controls. Such breakage was only observed in one wire from among all the 16 wrapped specimens; and
5. The average residual bond for the CFRP and GFRP were similar and largely unaffected by exposure. Adhesives used by both systems were durable.

In practice, if piles were wrapped at the time of installation, their performance would be vastly superior because the FRP would serve as a barrier to the ingress of chloride and significantly delay the onset of corrosion. Electrochemical measurements clearly indicate, however, that there are sufficient oxygen and moisture within the wrapped region to sustain the corrosion inside the wrap. This can be remedied by integrating a cathodic protection system within the wrap. Such development work is currently underway.

ACKNOWLEDGMENTS

This study was performed in cooperation and funding from the State of Florida and the U.S. Department of Transportation. This support is gratefully acknowledged. The assistance and guidance of J. Garcia and S. Womble from the FDOT are gratefully acknowledged. The authors are indebted to E. Fyfe, Fyfe & Co, LLC, for providing materials used in the testing. The authors also thank SDR Engineering, Tallahassee, Fla., for its contribution.

REFERENCES

1. Tarricone, P., "Composite Sketch," *Civil Engineering*, ASCE, May 1995, pp. 52-55.
2. Alampalli, S., "Reinforced Polymers for Rehabilitation of Bridge Columns," *Proceedings of the 5th National Workshop on Bridge Research in Progress*, Oct. 2001, pp. 39-41.
3. Sen, R., "Advances in the Application of FRP for Repairing Corrosion Damage," *Progress in Structural Engineering and Materials*, V. 5, No. 2, 2003, pp. 99-113.
4. Sheikh, S.; Pantazoupoulou, S.; Bonacci, J.; Thomas, M.; and Hearn, N., "Repair of Delaminated Circular Pier Columns with Advanced Composite Materials," *Ontario Joint Transportation Research Report* No. 31902, Ministry of Transportation of Ontario, Aug. 1997, 75 pp.
5. Neale, K. W., and Labossiere, P., "Fiber Composite Sheets in Cold Climate Rehab," *Concrete International*, V. 20, No. 6, June 1998, pp. 22-24.
6. Bonacci, J., "Rehabilitation of Corrosion-Damaged RC Infrastructure Using Externally Bonded FRP," *Proceedings of ACMBS 2000*, CSCE, Montreal, Quebec, Canada, 2000, pp. 561-568.
7. Baiyasi, M., and Harichandran, R., "Corrosion and Wrap Strains in Concrete Bridge Columns Repaired with FRP Wraps," *Paper* No. 01-2609, 80th Annual Meeting, Transportation Research Board, Washington, D.C., 2001.
8. Debaiky, A.; Green, M.; and Hope, B., "Carbon Fiber-Reinforced Polymer Wraps for Corrosion Control and Rehabilitation of Reinforced Concrete Columns," *ACI Materials Journal*, V. 99, No. 2, Mar.-Apr. 2002, pp. 129-137.
9. Wootton, I.; Spainhour, L.; and Yazdani, N., "Corrosion of Steel Reinforcement in CFRP Wrapped Concrete Cylinders," *Journal of Composites for Construction*, V. 7, No. 4, 2003, pp. 339-347.

10. Wheat, H. G.; Jirsa, J. O.; and Fowler, D. W., "Monitoring Corrosion Protection Provided by Fibre Reinforced Composites," *International Journal of Materials and Product Technology*, V. 23, No. 3/4, 2005, pp. 372-388.

11. Mullins, G.; Sen, R.; Torres-Acosta, A.; Goulish, A.; Suh, K.; Pai, N.; and Mehrani, A., "Load Capacity of Corroded Pile Bents," *Final Report* submitted to the Florida Department of Transportation, Sept. 2001, 327 pp.

12. Suh, K. S.; Mullins, G.; Sen, R.; and Winters, D., "Use of FRP for Corrosion Strengthening Applications in a Marine Environment," *Final Report* submitted to Florida/U.S. Department of Transportation, Tallahassee, Fla., Oct. 2005, 406 pp.

13. Bazinet, S.; Cereone, L.; and Worth, F., "Composite FRP Moves into Underwater Repair Applications," *SAMPE Journal*, V. 39, No. 3, May-June 2003, pp. 8-16.

14. Mullins, G.; Sen, R.; Suh, K.; and Winters, D., "Underwater FRP Repair of Prestressed Piles in the Allen Creek Bridge," *Journal of Composites for Construction*, ASCE, V. 9, No. 2, 2005, pp. 136-146.

15. Sen, R.; Mullins, G.; Suh, K. S.; and Winters, D., "FRP Application in Underwater Repair of Corroded Piles," *7th International Symposium on Fiber-Reinforced (FRP) Polymer Reinforcement for Concrete Structures*, SP-230, C. Shield, J. Busel, S. Walkup, and D. Gremel, eds., V. 2, American Concrete Institute, Farmington Hills, Mich., 2005, pp. 1139-1156.

16. Mullins, G.; Sen, R.; Suh, K.; and Winters, D., "A Demonstration of Underwater FRP Repair," *Concrete International,* V. 28, No. 1, Jan. 2006, pp. 70-73.

17. Berver, E.; Jirsa, J.; Fowler, D.; Wheat, H.; and Moon, T., "Effects of Wrapping Chloride Contaminated Concrete with Fiber-Reinforced Plastics," FHWA/TX-03/1774-2, University of Texas at Austin, Austin, Tex., Oct. 2001, 112 pp.

18. *Concrete Repair Manual*, 2nd Edition, V. 1, American Concrete Institute, Farmington Hills, Mich., 2003, p. 464.

19. ASTM D 4541, "Standard Test Method for Pull-Off Strength of Coatings Using Portable Adhesion Testers," ASTM International, West Conshohocken, Pa., 2002, 13 pp.